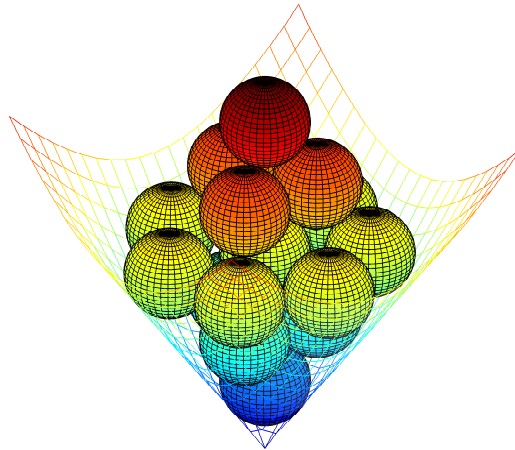


# CHALMERS



## Modulation Optimization for Noncoherent Optical Systems

JOHNNY KAROUT

Communication Systems Group  
Department of Signals and Systems  
CHALMERS UNIVERSITY OF TECHNOLOGY  
Gothenburg, Sweden 2011



Thesis for the degree of Licentiate of Engineering

---

**Modulation Optimization for Noncoherent  
Optical Systems**

JOHNNY KAROUT



**CHALMERS**

Communication Systems Group  
Department of Signals and Systems  
Chalmers University of Technology

Gothenburg, 2011

Karout, Johnny  
Modulation Optimization for Noncoherent Optical Systems.

Department of Signals and Systems  
Technical Report No. R010/2011  
ISSN 1403-266X

Communication Systems Group  
Department of Signals and Systems  
Chalmers University of Technology  
SE-412 96 Gothenburg, Sweden  
Telephone: + 46 (0)31-772 1000

Copyright ©2011 Johnny Karout  
except where otherwise stated.  
All rights reserved.

This thesis has been prepared using L<sup>A</sup>T<sub>E</sub>X.

*Front Cover:* The figure on the front cover is a 16-level single-subcarrier constellation optimized for peak power (See [Paper C] for details).

Printed by Chalmers Reproservice,  
Gothenburg, Sweden, August 2011.

*In memory of my father*

“Only those who will risk going too far can possibly find out  
how far one can go.”  
T. S. Eliot



# Abstract

There has been a significant improvement in high-speed electronics and optical components over the past few years, and this is one of the key enabling factors for high data rate transmission. Moreover, multi-level modulation formats, which encode information onto the carrier's amplitude and phase, are necessary to increase the spectral efficiency of communication systems. For short-haul low cost optical links, as the ones used in data centers and access networks for example, non-coherent optical communication with directly modulated lasers and direct detection receivers is more cost-effective than using coherent communication systems. Such types of noncoherent communications use the intensity of the optical carrier to carry information. These systems can be modeled as an additive white Gaussian noise channel with input constrained to being nonnegative. Subcarrier modulation, a concept studied in the wireless infrared communications context, allows the use of in-phase and quadrature phase (I/Q) modulation formats for such types of noncoherent optical systems.

We propose a novel quaternary subcarrier modulation format in [Paper A] which is a hybrid between on-off keying (OOK) and ternary phase-shift keying. At asymptotically high signal-to-noise ratios, this hybrid format offers a 1.2 dB average electrical power gain and 0.6 dB average optical power gain compared to OOK, making it the most power-efficient format for noncoherent optical systems with a spectral efficiency of 1 bit/s/Hz. However, for systems that are limited by laser nonlinearities, we show that OOK is the best choice at this spectral efficiency.

In [Paper B], we complement the theoretical results obtained in [Paper A] by carrying out an experimental link analysis, thus comparing the different modulation formats with spectral efficiency of 1 bit/s/Hz. In agreement with the theory, the proposed modulation format is more power efficient in terms of average optical power compared to the other modulation formats under study. However, the

gain comes at the cost of higher transceiver complexity. In addition, we study the impact of propagation in multimode fiber for different fiber lengths, and the analysis shows that all the studied modulation formats have a similar performance penalty due to the modal dispersion present in multimode fibers.

The agreement of theory with the obtained experimental results motivated us to optimize higher-level modulation formats for different power measures. In [Paper C], we propose a set of 4-, 8-, and 16-level single-subcarrier modulation formats for noncoherent optical systems which are optimized for average electrical, average optical, and peak power. In the absence of error-correcting codes, the optimized modulation formats offer a gain ranging from 0.6 dB to 3 dB compared to the best known formats. It was also noticed that modulation formats optimized for peak power perform well in average-power limited systems. When capacity-achieving error-correcting codes are present, the obtained modulation formats offer a gain ranging from 0.3 dB to 1 dB compared to previously known formats. The modulation formats optimized for average optical power have a better performance, except in peak-power limited systems. We also analyze and design modulation formats which are optimized for the low signal-to-noise ratio regime when capacity-achieving codes are used.

**Keywords:** Direct detection, fiber-optical communications, free-space optical communications, infrared communications, intensity modulation, lattice codes, mutual information, noncoherent communications, sphere packing.

# List of Included Publications

This thesis is based on the following papers:

- [A] J. Karout, E. Agrell, and M. Karlsson, “Power efficient sub-carrier modulation for intensity modulated channels,” *Optics Express*, vol. 18, no. 17, pp. 17913–17921, Aug. 2010.
- [B] K. Szczerba, J. Karout, P. Westbergh, E. Agrell, M. Karlsson, P. Andrekson, and A. Larsson, “Experimental comparison of modulation formats in IM/DD links,” *Optics Express*, vol. 19, no. 10, pp. 9881–9889, May 2011.
- [C] J. Karout, E. Agrell, K. Szczerba, and M. Karlsson, “Optimizing constellations for noncoherent optical communication systems,” submitted to *IEEE Transactions on Information Theory*, Jun. 2011.



# Contents

<b>Abstract</b>	<b>i</b>
<b>List of Included Publications</b>	<b>iii</b>
<b>Acknowledgements</b>	<b>ix</b>
<b>Acronyms</b>	<b>xi</b>
<b>I Overview</b>	<b>1</b>
<b>1 Introduction</b>	<b>1</b>
<b>2 Digital Modulation and Demodulation Theory</b>	<b>5</b>
2.1 Signal Space Analysis . . . . .	6
2.2 I/Q Modulation and Demodulation . . . . .	8
2.2.1 Transmitter . . . . .	8
2.2.2 Receiver . . . . .	9
2.3 Sphere Packing . . . . .	10
<b>3 Optical Communications</b>	<b>13</b>
3.1 Coherent Optical Systems . . . . .	14
3.2 Noncoherent Optical Systems . . . . .	15
<b>4 Single-Subcarrier Noncoherent Modulation</b>	<b>20</b>
4.1 Single-Subcarrier Modulation Signal Space . . . . .	21
4.2 Figures of Merit . . . . .	24
4.3 Constellation Optimization . . . . .	27
4.4 Experimental Verification . . . . .	28

<b>5 Contributions</b>	<b>31</b>
5.1 Included Publications . . . . .	31
5.2 Other Contributions . . . . .	32
<b>References</b>	<b>34</b>
<b>II Included papers</b>	<b>41</b>
<b>A Power Efficient Subcarrier Modulation for Intensity Modulated Channels</b>	<b>A1</b>
A.1 Introduction . . . . .	A2
A.2 System Model . . . . .	A4
A.3 Investigated Modulation Schemes . . . . .	A5
A.4 Performance Investigation . . . . .	A6
A.5 Conclusion . . . . .	A11
References . . . . .	A11
<b>B Experimental Comparison of Modulation Formats in IM/DD Links</b>	<b>B1</b>
B.1 Introduction . . . . .	B2
B.2 Theoretical Background . . . . .	B3
B.3 Experimental Setup . . . . .	B6
B.4 Experimental Results . . . . .	B7
B.5 Conclusions and Future Work . . . . .	B11
References . . . . .	B12
<b>C Optimizing Constellations for Noncoherent Optical Communication Systems</b>	<b>C1</b>
C.1 Introduction . . . . .	C2
C.2 System Model . . . . .	C5
C.3 Signal Space Model . . . . .	C7
C.3.1 Performance Measures . . . . .	C8
C.3.2 Single-Subcarrier Modulation Formats . . . . .	C10
C.4 Constellation Optimization . . . . .	C12
C.4.1 Optimized Constellations . . . . .	C13
C.4.2 Previously Known Constellations . . . . .	C17
C.5 Performance Analysis . . . . .	C18
C.5.1 Symbol Error Rate . . . . .	C18

C.5.2	Asymptotic Power Efficiency . . . . .	C22
C.5.3	Mutual Information vs. SNR . . . . .	C25
C.5.4	Mutual Information in the Wideband Regime .	C27
C.6	Conclusions . . . . .	C32
Appendix A	. . . . .	C33
References	. . . . .	C35



# Acknowledgements

One of the best moments in life is when you feel that you have the chance to thank the people who have contributed to your daily life in one way or another, and now it is my chance to thank each and every person without whom this work would not have been possible.

Prof. Erik Agrell, working with you is such a pleasure, and I am very grateful for giving me this opportunity of working in such a stimulating environment. The way you do research, the openness to new ideas, your critical thinking, and the confidence you put in your students are things I really appreciated and learned from. I am also grateful to my co-supervisor, Prof. Magnus Karlsson, for all the nice discussions and the support he has provided. Interacting with both of you has been such a wonderful experience!

I would also like to thank each and every member of the fiber optic communications research center (FORCE) for making it such a nice research environment. Just by being there and talking to people with different backgrounds is such a great learning opportunity. Special thanks to Assistant Prof. Henk Wymeersch and for all the new research topics he introduced me to. I will also take the opportunity to thank Assistant Prof. Pontus Johannisson for the many fruitful discussions we had. And of course, I would like to thank Krzysztof Szczerba who is working on the same research topic, but from an experimental viewpoint. Collaborating with you helped me a lot in understanding the different hardware impairments. Keep up the good work man!

Many thanks to Prof. Erik Ström for all his efforts to making the experience of being in the Communication Systems and Information Theory group more and more interesting. I would also like to thank the current and former members of the group. In particular, I would like to thank Prof. Arne Svensson, Prof. Thomas Eriksson, Associate

Prof. Tommy Svensson, Dr. Mats Rydström, and each of the Assistant Professors Giuseppe Durisi, Fredrik Brännström, and Alexandre Graell i Amat for all the informal discussions. I am also thankful to Dr. G. Garcia, Dr. A. Tahmasebi, Dr. A. Alvarado, Dr. L. Svensson, Lotfollah, Kasra, Nima, Ali, Mohammad, Tilak, Rajet, Haiying, Behrooz, Katrin, Jingya, Yutao, Wei, Sun, Mikhail, Dr. Mehrpouyan, and Dr. Sen for being good and friendly colleagues. Gratitudes to Agneta, Natasha, and Lars for all their help, and to Dr. Ouais for the continuous support. I would also like to thank Livia, Astrid, Elena, Panagiota, Tomas, Marie, Johan, Peter, Walid, and Roger for being great friends! A special thanks goes to Maya for being a good source of support and inspiration!

Finally, I would like to thank my family for all the support they have given me over the years. Mom, a thank you is just not enough! Simon, Peter, and Roger, I am really lucky to be surrounded by brothers like you. Thank you all! And of course, my sister and closest friend Randa, *hmmm* I don't know what to say! What you have done over the years is something I would never ever forget.

*Johnny Karout*  
*Gothenburg, June 2011*

# Acronyms

AWGN	Additive White Gaussian Noise
BPSK	Binary Phase-Shift Keying
DC	Direct Current
DMT	Discrete Multitone
DP-QPSK	Dual-Polarization QPSK
FDM	Frequency Division-Multiplexing
IM/DD	Intensity-Modulated Direct-Detection
I/Q	In-phase and Quadrature Phase
LO	Local Oscillator
LPF	Low-Pass Filter
MAP	Maximum A Posteriori
MF	Matched Filter
ML	Maximum Likelihood
MMF	Multimode Fiber
<i>M</i> -PAM	Multilevel Pulse Amplitude Modulation
<i>M</i> -PSK	Multilevel Phase-Shift Keying
<i>M</i> -QAM	Multilevel Quadrature Amplitude Modulation
MSM	Multiple-Subcarrier Modulation
MZM	Mach-Zehnder Modulator

OFDM	Orthogonal Frequency-Division Multiplexing
OOK	On-Off Keying
PD	Photodiode
QPSK	Quadrature Phase-Shift Keying
RIN	Relative Intensity Noise
SCM	Subcarrier Modulation
SER	Symbol Error Rate
SNR	Signal-to-Noise Ratio
VCSEL	Vertical-Cavity Surface-Emitting Laser
VOA	Variable Optical Attenuator

Part I

Overview



# Chapter 1

## Introduction

Claude Elwood Shannon, with his landmark paper in 1948 [1] and the included theory underlying digital communications and storage, paved the way for the information era that we are living in. This theory deals with the fundamental limits of storing and communicating data, and it is what he called *information theory*. Since then, efforts have been devoted to approach such limits while providing a good trade-off between the spectral efficiency, power efficiency, and complexity/cost of a communication system as shown in Fig. 1.1. However, this trade-off becomes tricky, especially with the many emerging bandwidth hungry applications such as data centers, storage area networks, cloud computing, high-performance computing, etc. Therefore, it is desirable to have a low cost system which supports the increasing amounts of data traffic without drastically increasing the power consumption.

In the 1950s, it was realized that supporting huge data rates is feasible by using an optical carrier instead of a microwave carrier to carry information [2, Ch. 1]. This is due to the high carrier frequency (around 100 THz) of light, which can carry a huge amount of information. Moreover, the advancement in optical glass fibers and their lower losses compared to copper cables made fiber optical communications, specifically with the use of single-mode fibers, prevalent in long-haul transmission. In order to improve the spectral efficiency of such systems, coherent communications where information is encoded onto the amplitude and phase of the optical carrier can be used together with the two available polarizations of the carrier wave. On the other hand, short low-cost links require affordable optics such as

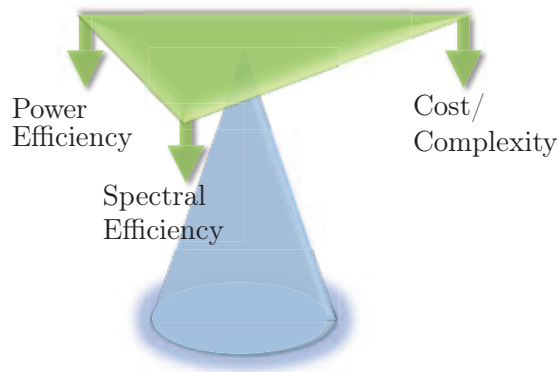


Figure 1.1: Trade-offs in a communication system.

noncoherent optical transceivers. As opposed to coherent communications, only the intensity of the optical carrier is used to carry information, and the envelope of the received signal is detected at the receiver. Such types of noncoherent systems are known as *intensity-modulated direct-detection* (IM/DD) systems. These are prevalent in wireless optical communications [3–5] and in short-haul fiber links, especially those with multimode fibers due to their low installation costs. Examples of applications which use IM/DD are local area networks, storage area networks, data centers, etc.

One way of improving the spectral efficiency of IM/DD systems is by using multilevel pulse amplitude modulation ( $M$ -PAM). However,  $M$ -PAM has a higher power penalty compared to on-off keying (OOK) [6]. Another alternative is the use of subcarrier modulation (SCM) studied in the wireless infrared communications context [3, Ch. 5] which allows the use of in-phase and quadrature phase modulation formats such as multilevel phase-shift keying ( $M$ -PSK) and multilevel quadrature amplitude modulation ( $M$ -QAM), i.e., the electrical subcarrier carries information on its amplitude and phase. The IM/DD channel differs from the conventional coherent channel by the fact that its input is constrained to being nonnegative. This is achieved by adding a direct current (DC) bias to the electrical signal carrying the information to be nonnegative. This biased electrical signal directly modulates a light source, e.g., laser diode, to generate an optical signal whose intensity is proportional to it. One option is

---

that the DC bias required to ensure the nonnegativity of the electrical waveform does not carry information [3, Ch. 5], [7, 8]. The second option is by allowing the DC bias to carry information thus improving the power efficiency. This is studied by varying the DC bias on a symbol-by-symbol basis in [9], and within the symbol interval in [10]. In [11], a signal space model for optical IM/DD channels is presented, and shaping regions which reduce the average and peak optical power are derived. These regions are used to design power-efficient lattice-based modulation formats.

The choice of modulation formats governs the complexity of the transceiver structure that should be used. Therefore, using lattice-based modulation formats which are characterized by their regular geometric structure reduce the complexity of the modulator and demodulator.

The aim of this work is to optimize IM/DD modulation formats for uncoded systems with and without confining them to a regular structure such as a lattice. We propose a set of 4-, 8-, and 16-level single-subcarrier modulation formats which are optimized for average electrical, average optical, and peak power. These optimization criteria are all relevant since they help in assessing the overall power consumption [12], the conformity to skin- and eye-safety standards in wireless optical links [3, Ch. 5], [4, 11], and the tolerance against the nonlinearities present in the system [13] (see Sec. 4.2 for details). In addition, laboratory experiments were carried out to see how far the experimental results are from theory. We also analyze the performance of the obtained modulation formats in terms of mutual information in order to predict their performance in the presence of capacity-achieving error-correcting codes. In terms of mutual information, we analytically optimize modulation formats in the low signal-to-noise ratio (SNR) regime and compare them with the other obtained formats.

The structure of this thesis is organized as follows. Chapter 2 introduces the signal space analysis in digital communications, and presents the modulation and demodulation for in-phase and quadrature phase modulation formats in the presence and absence of phase information at the receiver. Chapter 3 introduces optical communications with a focus on noncoherent communications where the system model is presented. In Chapter 4, single-subcarrier modulation for

IM/DD channels will be introduced, where the signal space and figures of merit will be presented. The optimization problem will be formulated followed by an example of the obtained constellations, together with the experimental laboratory setup that was performed. Finally, in Chapter 5, the contributions will be summarized.

## Chapter 2

# Digital Modulation and Demodulation Theory

It is a remarkable fact that the earliest form of electrical communication was digital with the invention of telegraphy by Samuel Morse in 1837 [14, Ch. 1]. Even with this early form of communication, source coding was used due to the fact that frequent letters of the English alphabet were represented by short sequences of codewords (dots and dashes), whereas less frequent letters were represented by longer codewords. It took almost a century to realize digital communications the way we know it today. This started with the work of Nyquist in 1924 who investigated the maximum rates that can be used over a bandlimited telegraph channel without intersymbol interference. This was extended by Hartley in 1928 for multilevel signaling. Another milestone is the work of Wiener in 1942, where he investigated the problem of estimating the desired signal at the receiver in the presence of additive noise [14, Ch. 1]. Then followed “the” milestone with the work of Shannon and his landmark paper titled “A Mathematical Theory of Communication” in 1948 [1]. Shannon established the mathematical foundations for information transmission and derived the fundamental limits of digital communication systems, given by the *channel capacity*. Since then, the channel capacity and the underlying theory have served as a benchmark for all the new advances in the area of digital communications.

This chapter focuses on the additive white Gaussian noise (AWGN) channel model. The signal space, which allows the representation of

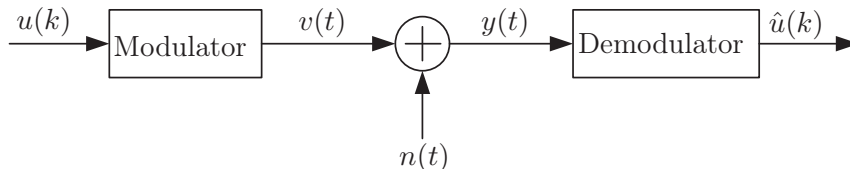


Figure 2.1: The model of a communication system.

the signals used for transmission geometrically, is introduced. This will be the basis for understanding the specific class of in-phase and quadrature phase (I/Q) modulation formats which are widely spread. Sec. 2.2 presents the I/Q modulator and the two classes of demodulation, coherent and noncoherent, where the former has complete knowledge of the carrier phase, and the latter has no carrier phase knowledge. Finally, Sec. 2.3 introduces the guidelines for designing power-efficient modulation formats, and how this problem can be reformulated as a sphere packing problem.

## 2.1 Signal Space Analysis

Fig. 2.1 shows a schematic of a communication system consisting of a modulator which maps each symbol  $u(k)$  at instant  $k$  to a waveform  $v(t)$  belonging to the signaling set  $S = \{s_0(t), s_1(t), \dots, s_{M-1}(t)\}$ , where  $M$  is the size of the signaling set. The symbols  $u(k)$  are modeled as an ergodic process uniformly distributed over  $\{0, 1, \dots, M-1\}$ . In this section, we will only consider the transmission of a single symbol. The generated waveform  $v(t)$  propagates through the transmission medium, and the signal at the receiver can be written as

$$y(t) = v(t) + n(t), \quad (2.1)$$

where  $n(t)$  is a zero-mean Gaussian process with double-sided power spectral density  $N_0/2$  which models the thermal noise generated at the receiver. This is then followed by the demodulation of  $y(t)$  which yields  $\hat{u}(k)$ , an estimate of  $u(k)$ . The demodulator is a correlator or matched filter receiver, which minimizes the symbol error rate (SER) at a given SNR [15, Sect. 4.1].

For evaluating the performance of communication systems in terms of their error probability, the continuous-time signals might be tedious

to start with. Therefore, using the signal space analysis developed by Kotelnikov [16], and later expanded by Wozencraft and Jacobs [17] helps in portraying the continuous-time signals as points in Euclidean space, which makes the error probability calculations feasible. In addition, viewing the signaling set as constellation of points in Euclidean space provides a better understanding and an intuition on how to better design signaling sets.

By defining a set of orthonormal basis functions  $\phi_k(t)$  for  $k = 1, 2, \dots, N$  and  $N \leq M$ , each of the signals in  $S$  can be represented as

$$s_i(t) = \sum_{k=1}^N s_{i,k} \phi_k(t), \quad (2.2)$$

for  $i = 0, \dots, M-1$ , where  $\mathbf{s}_i = (s_{i,1}, s_{i,2}, \dots, s_{i,N})$  is the vector representation of  $s_i(t)$  with respect to the aforementioned basis functions. Therefore, the constellation representing the signaling set  $S$  can be written as  $\Omega = \{\mathbf{s}_0, \mathbf{s}_1, \dots, \mathbf{s}_{M-1}\}$ . In a similar fashion, the noise  $n(t)$  can be expressed as

$$n(t) = \sum_{k=1}^N n_k \phi_k(t) + w(t), \quad (2.3)$$

where  $w(t)$  is the noise component outside the space spanned by the basis functions in which all the signals in the signaling set belong to. However, the Theorem of Irrelevance states that the noise outside the dimensions of the signals has no effect on the detection process, and thus no effect on the overall performance [18, p. 52]. Therefore, without loss of generality, the vector representation of the noise component which affects the detection process is

$$\mathbf{n} = (n_1, n_2, \dots, n_N). \quad (2.4)$$

With this representation, the continuous-time channel model in (2.1) can be represented by the discrete-time vector model

$$\mathbf{y} = \mathbf{v} + \mathbf{n}, \quad (2.5)$$

where  $\mathbf{v} \in \Omega$  is the transmitted vector, and  $\mathbf{n}$  is a Gaussian random vector with independent elements, zero mean, and variance  $N_0/2$  per dimension.

For instance, by using the signal space analysis and the fact that the noise is AWGN, the optimum detector, which is based on the maximum a posteriori (MAP) criterion or the maximum likelihood (ML) criterion when the transmitted signals are equally probable, outputs the signal vector in  $\Omega$  that is closest in Euclidean distance to the received signal vector  $\mathbf{y}$ .

## 2.2 I/Q Modulation and Demodulation

In this section, we consider the modulation and demodulation of a pulse train using I/Q formats such as  $M$ -PSK and  $M$ -QAM. These formats give access to both the electrical carrier's amplitude and phase. The signal space for such type of modulation formats is a two-dimensional space spanned by the orthonormal basis functions [18, Sec. 3.2.3]

$$\phi_1(t) = \sqrt{\frac{2}{T_s}} p(t) \cos(2\pi ft), \quad (2.6)$$

$$\phi_2(t) = \sqrt{\frac{2}{T_s}} p(t) \sin(2\pi ft), \quad (2.7)$$

where  $T_s$  is the symbol time,  $f$  is the carrier frequency, and  $p(t)$  is a unit-energy baseband pulse with bandwidth  $W$  and  $f > W$ .

Even if  $p(t)$  is not a bandlimited pulse, e.g., a rectangular pulse for  $0 < t \leq T_s$ , the orthogonality criterion can still be satisfied if  $f$  is a multiple of  $1/T_s$ . This is the idea behind the subcarrier modulation formats which will be discussed in Ch. 4.

### 2.2.1 Transmitter

Fig. 2.2 shows the setup of an I/Q modulator. It consists of multiplying the in-phase and quadrature baseband pulse trains

$$I(t) = \sum_k s_{u(k),1} p(t - kT_s)$$

and

$$Q(t) = \sum_k s_{u(k),2} p(t - kT_s)$$

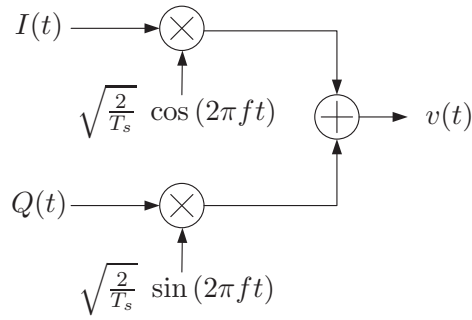


Figure 2.2: I/Q modulator.

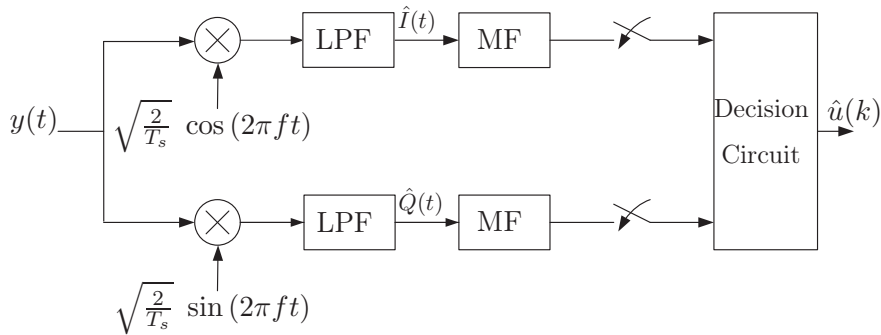


Figure 2.3: Coherent I/Q demodulator.

with  $\sqrt{2/T_s} \cos(2\pi ft)$  and  $\sqrt{2/T_s} \sin(2\pi ft)$ , respectively. The sum of these two branches yields the passband transmitted waveform

$$v(t) = \sqrt{\frac{2}{T_s}} [I(t) \cos(2\pi ft) + Q(t) \sin(2\pi ft)], \quad (2.8)$$

where information is carried onto its amplitude and phase.

### 2.2.2 Receiver

In the presence of perfect carrier synchronization, the receiver can make use of the phase reference information to demodulate the received signal. This is known as coherent demodulation and is shown in Fig. 2.3. The receiver mixes the noisy received signal  $y(t) = v(t) + n(t)$  with  $\sqrt{2/T_s} \cos(2\pi ft)$  and  $\sqrt{2/T_s} \sin(2\pi ft)$ , i.e., the in-phase and

quadrature phase sinusoidal references, generated by a local oscillator (LO) at the receiver. Low-pass filtering (LPF) of the output results in  $\hat{I}(t)$  and  $\hat{Q}(t)$ , which are the estimates of the baseband signals  $I(t)$  and  $Q(t)$ . These are fed to a bank of filters matched to the pulse  $p(t)$ , denoted as MF, which is then followed by sampling and a decision circuit which outputs the symbols closest in signal space to the received ones.

However, in scenarios where the phase reference information is unavailable at the receiver, cross-talk between the in-phase and quadrature phase arms is unavoidable. The amount of cross-talk depends on the phase error value between the locally generated and the incoming phase [15, p. 309]. In such scenarios, noncoherent detection where the receiver makes no use of the phase reference is an attractive approach. For each  $i = 0, 1, \dots, M - 1$ , the optimum demodulator correlates the received signal  $y(t)$  with  $s_i(t)$  and a  $90^\circ$  phase-shifted version of  $s_i(t)$  over the symbol period [19, Sec. 6.7]. The metric for signal  $i$  is obtained by adding the squares of these two correlations, and the signal resulting in the largest metric is the optimum choice. This type of demodulator is suitable, for example, when frequency-shift keying formats are deployed. However, if the signals being transmitted are the same but differ with a phase-shift, e.g.,  $M$ -PSK formats, the resulting envelopes are the same. This causes ambiguity at the receiver on which signal to decide upon. The ambiguity is also present when  $M$ -QAM formats are used.

## 2.3 Sphere Packing

The symbol error rate serves as a good measure to compare different modulation formats. However, the exact value might be difficult to compute depending on the constellation geometry, number of levels, and number of dimensions. For this reason, the standard union bound in [15, Eq. (4.81)] which is based on the pairwise error probabilities can be used to upperbound the SER. This union bound can be approximated as

$$P_s \approx \frac{2K}{M} Q \left( \sqrt{\frac{d_{\min}^2}{2N_0}} \right), \quad (2.9)$$

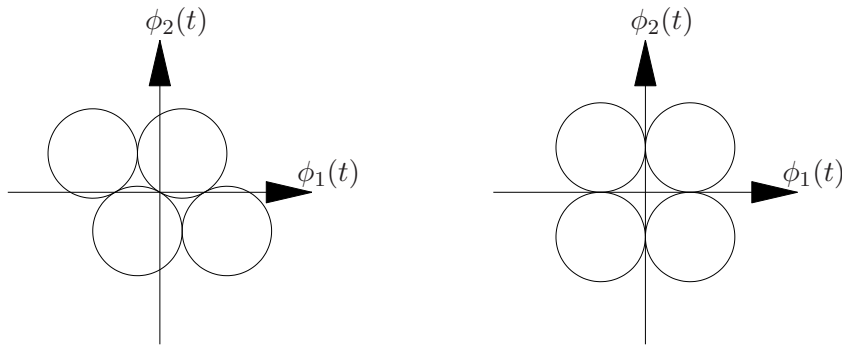


Figure 2.4: 4-level constellation optimized for average energy (left), and for average and peak energy simultaneously (right).

where  $K$  is the number of distinct signal pairs  $(s_i(t), s_j(t))$  with  $i < j$  for which  $\int (s_i(t) - s_j(t))^2 dt = d_{\min}^2$ , and  $d_{\min}$  is the minimum distance between the constellation points. This approximation approaches the true SER at high SNR. From (2.9), it can be inferred that a good modulation format is the one which minimizes the energy, whether average or peak, while keeping  $d_{\min}$  constant.

As a consequence, designing asymptotic power-efficient modulation formats can be reformulated as a sphere packing problem with the attempt of finding the densest packing of  $M$   $N$ -dimensional spheres, i.e., two-dimensional for I/Q modulation formats. The coordinates of the sphere centers represent the constellation points. If the average energy is the limiting factor in a communication system, then the objective would be to find the packing which minimizes the average squared distance of the center of the spheres from the origin. However, if the peak energy is the constraint, then the densest packing is translated to finding the constellation which minimizes the maximum distance of the sphere centers from the origin.

Even though such problems can be well formulated mathematically, it is rather difficult to obtain an analytical solution. Therefore, numerical optimization techniques are used to find the best possible packing. This has been explored extensively for the AWGN channel with coherent detection for different power constraints, whether average or peak power [20–24]. The drawback is the lack of geometric

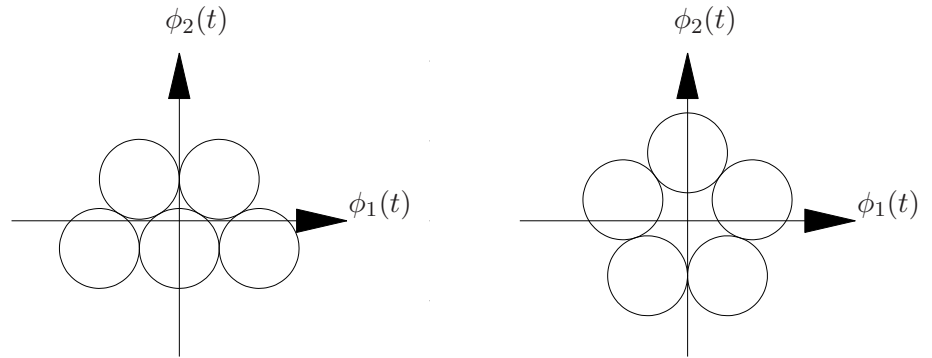


Figure 2.5: 5-level constellation optimized for average energy (left), and for peak energy (right).

regularity, which increases the modulator and demodulator complexity. On the other hand, *lattice codes*, which are a finite set of points selected out of an  $N$ -dimensional lattice, is another approach which has been extensively used in the construction of multilevel modulation formats [25–27]. Even though this approach might not guarantee optimality, it simplifies the modulator and demodulator due to the regular structure of a lattice.

For the two-dimensional space presented in Sec. 2.2, the best packing which provides the minimum average energy is always a subset of the hexagonal lattice as shown in [23], whereas the packings optimized for providing the minimum peak energy have more irregular structures as can be found in [28]. The exception to this is shown in Fig. 2.4 where the two 4-level constellations presented have the same minimum average energy among other possible constellations, despite the fact that the QPSK constellation in Fig. 2.4 (right) is not a subset of the hexagonal lattice. However, the QPSK constellation offers the lowest peak energy for  $M = 4$ . On the other hand, Fig. 2.5 shows two 5-level constellations where the hexagonal lattice-based constellation (left) is optimized for average energy, and the constellation whose points lie on a circle is optimized for peak energy [29].

## Chapter 3

# Optical Communications

Since the 1950s, the term *optical communications* is always accompanied with the huge amounts of data rates that can be reached together with the long transmission distances when fibers are used as the transmission medium. However, optical communication has been used way earlier than the 1950s. Of the earliest forms of optical communications are the fire beacons mentioned in the *Iliad* by Homer which were used to transmit information in the siege of Troy which took place in approximately 1184 BC [5, Sec. 1.1]. Since then, some of the key milestones that the technology has passed through are the invention of the optical telegraph by Chappe in the 1790s, the photophone by Bell and Tainter in the 1880s [5, Sec. 1.1], the optical glass fibers in the 1950s, and the laser in 1960 [2, Sec. 1.1]. Another key milestone is the silica fiber proposed by Kao and Hockham in 1966 that led to a breakthrough in fiber optics where long distance transmission was shown to be feasible [30]. Today, a massive network of fiber optic cables exists worldwide [2, Sec. 1.1]. In 1979, wireless optical communication was pioneered by Gfeller and Bapst with the use of diffuse emissions in the infrared band [31]. Since then, many efforts have been focusing on transmitter and receiver design, channel modeling, and impairment compensation in attempt to boost the data rates even more.

In this chapter, coherent optical systems which give access to both the amplitude and phase of the optical carrier will be introduced. For such type of systems, optimizing modulation formats is very similar to that of coherent communication systems for AWGN channels as

in the previous chapter. This will be followed by introducing the noncoherent optical communications where information is transmitted only onto the intensity of the optical carrier. In the next chapter, noncoherent communications will be covered in more depth.

### 3.1 Coherent Optical Systems

Multilevel modulation formats, with their ability to increase the spectral efficiency of a communication system, have motivated the use of coherent optical transceivers. Such coherent transceivers enable the modulation of data independently onto the I and Q quadratures of each of the two polarizations of an electromagnetic carrier wave. Therefore, all the four degrees of freedom can be used to send information. For example, modulation formats such as binary phase-shift keying (BPSK) use only one degree of freedom, whereas I/Q modulation formats such as quadrature phase-shift keying (QPSK) use two degrees of freedom. In order to use all the four degrees of freedom, I/Q modulation formats in the two polarizations should be used. An example of such a modulation format is the dual-polarization QPSK (DP-QPSK) which was experimentally tested in a real-time setup in [32].

A transmitter consists of a light source and an optical modulator. There are many possible structures to realize such an optical modulator [33]. An example is when the optical modulator block consists of both an amplitude and a phase modulator in series. Another example is by using an I/Q modulator with orthogonal optical carriers on the two arms, where each arm consists of an amplitude modulator such as a Mach-Zehnder modulator (MZM) for example, and the transmitted signal is the combined output of the two arms.

The receiver in general consists of photodetectors, an LO, and an electrical demodulator. The LO is necessary to generate the in-phase and quadrature phase reference, which will be fed to the photodetectors in the two polarizations. The output of the photodetectors is the electrical in-phase and quadrature phase components, which are further processed to extract the information bits that were transmitted.

A coherent optical fiber system using optical amplifiers can be well approximated by an AWGN channel model provided that dispersion and nonlinearity are negligible [34–36]. As a result, all the theory and

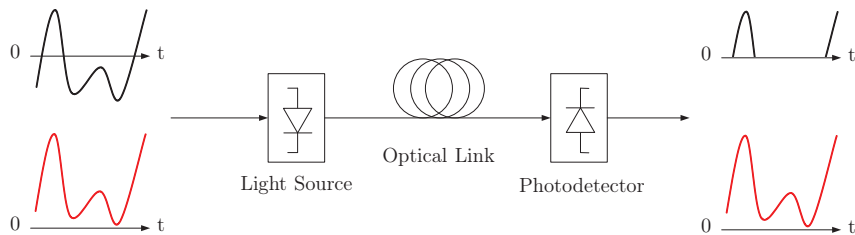


Figure 3.1: The black and red signals are to be transmitted over an IM/DD channel. The red signal is nonnegative, and can therefore be transmitted successfully as opposed to the black signal.

results obtained for the conventional electrical AWGN channel with the basis functions presented in (2.6) and (2.7) can be applied. This includes power-efficient modulation formats as a result of the densest sphere packing problems explored in [20–23] or when lattice codes are used [25–27]. In addition, the problem of optimizing modulation formats for coherent optical systems in a four-dimensional space, i.e., the I and Q quadratures in both polarizations, has been investigated thoroughly in [24, 37–40].

## 3.2 Noncoherent Optical Systems

In systems where phase information is absent at the receiver, the classical modulation formats optimized for coherent optical communications or for the conventional AWGN electrical channel cannot be used to convey information. Examples of such systems include phase-noise limited systems, and noncoherent systems where information is encoded onto the amplitude of the carrier and the envelope of the received signal is detected at the receiver. The latter is prevalent in optical communication systems where the overall cost and complexity is a critical constraint. Such type of noncoherent systems are known as IM/DD systems. Applications using IM/DD are, for example, wireless optical communications [3–5], and short-haul fiber links present in, e.g., data centers and local area networks [41].

Fig. 3.1 depicts the passband structure of IM/DD systems. An electrical signal which contains the information directly drives a light

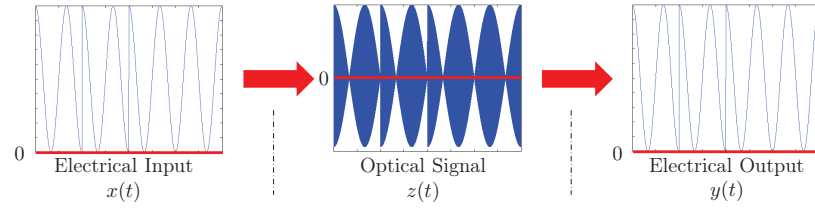


Figure 3.2: Biased BPSK over IM/DD channel. The waveforms  $x(t)$ ,  $z(t)$ , and  $y(t)$  are described below.

source such as a laser diode, where the intensity of the light generated, which is nonnegative at all times, is proportional to the input electrical signal. At the receiver, a photodetector outputs an electrical signal proportional to the optical power incident upon it. It can be seen from the figure that if the input electrical signal to the light source is nonnegative, the information to be sent can be successfully recovered at the receiver. Since the optical phase cannot be used to carry information, modulation formats such as OOK and  $M$ -PAM are suitable for IM/DD systems. The  $M$ -PAM for IM/DD systems is different from the conventional PAM since no negative amplitudes can be used [3, Eq. (5.8)]. However, if the information to be sent is modulated on an electrical subcarrier using any I/Q modulation format, e.g.,  $M$ -PSK or  $M$ -QAM, it could be transmitted successfully over an IM/DD channel on condition that this electrical signal is DC-biased to become nonnegative at all times. This gives the opportunity of designing modulation formats which could be more power efficient than OOK and  $M$ -PAM. This concept is known as *subcarrier modulation* and was described in the wireless infrared communications context in [3, Ch. 5]. Fig. 3.2 shows an example of information which is modulated on an electrical subcarrier using BPSK. After this message is biased, it directly modulates the light source. It should be noted that the envelope of the optical signal carries the electrical amplitude and phase. The envelope of the received optical signal is detected by the photodiode, which acts as a square-law detector. As a result, the electrical phase and amplitude of the transmitted signal is preserved. This will be followed by a BPSK demodulator to extract the transmitted information bits.

A complete passband transceiver for IM/DD systems is depicted

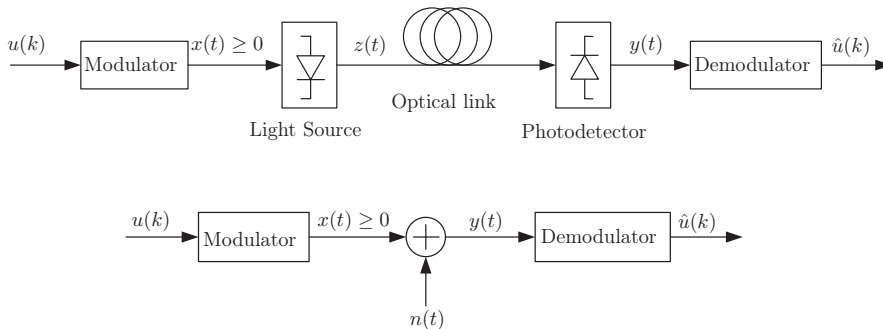


Figure 3.3: Passband transceiver of IM/DD systems (top). Baseband transceiver with constrained-input Gaussian channel (bottom).

in Fig. 3.3 (top). It consists of a modulator which maps the data symbols  $u(k)$  at instant  $k$  to a waveform belonging to the signaling set  $S = \{s_0(t), s_1(t), \dots, s_{M-1}(t)\}$ , where  $M$  is the size of the signaling set and  $s_i(t) = 0$  for  $t \notin [0, T_s)$  and  $i = 0, 1, \dots, M-1$ . The generated waveform

$$x(t) = \sum_{k=-\infty}^{\infty} s_{u(k)}(t - kT_s), \quad (3.1)$$

where  $T_s$  is the symbol period, is constrained to being real and non-negative. The baseband signal  $x(t)$  is composed of symbol waveforms shifted by integer multiples of  $T_s$ . This electrical nonnegative waveform  $x(t)$  directly modulates a light source. Therefore, the information is carried onto the envelope of the passband signal

$$z(t) = \sqrt{2cx(t)} \cos(2\pi f_o t + \theta), \quad (3.2)$$

i.e., onto the intensity of the optical field, where  $c$  represents the electro-optical conversion factor in watts per ampere (W/A) [42–44],  $f_o$  is the optical carrier frequency, and  $\theta$  is a random phase, uniformly distributed in  $[0, 2\pi)$ . It then propagates through the optical medium depicted as an optical fiber in Fig. 3.3 (top), which could be a free-space optical link in other applications. At the receiver, the photodetector detects the power of  $z(t)$  resulting in  $y(t)$ . This is then followed by the demodulation of  $y(t)$  which yields  $\hat{u}(k)$ , an estimate

of  $u(k)$ . The demodulator is a correlator or matched filter receiver, which minimizes the symbol error rate at a given SNR [15, Sect. 4.1].

Since the dominant channel impairment in most optical IM/DD systems is the thermal noise resulting from the optical-to-electrical conversion [45], [2, p. 155], the received electrical signal can be written as

$$\begin{aligned} y(t) &= \mathbb{L}\{rz^2(t)\} + n(t) \\ &= rcx(t) + n(t), \end{aligned} \quad (3.3)$$

where  $\mathbb{L}\{\cdot\}$  denotes a unit-gain low-pass filter that cancels the signal alias at twice the carrier frequency,  $r$  is the responsivity of the opto-electrical converter in A/W, and  $n(t)$  is a zero-mean Gaussian process with double-sided power spectral density  $N_0/2$ . Without loss of generality, we set  $rc = 1$ , which yields the simplified baseband model in Fig. 3.3 (bottom). The channel response is assumed to be ideal, thus not distorting the transmitted signal. This is to rule out the effect of the channel on the design of modulation formats. This model has been extensively studied in [3, Ch. 5], [4, 11, 46–48] in the wireless optical communications context. It is different from the conventional AWGN channel in Fig. 2.1 by the fact that the input  $x(t)$  is constrained to being nonnegative as opposed to the passband signal  $v(t)$  which could take on negative values. It should be noted that there exists no nonnegativity constraint on the signal  $y(t)$ . As in (2.5), the continuous-time channel model in (3.3) can be represented by the discrete-time vector model

$$\mathbf{y}(k) = \mathbf{x}(k) + \mathbf{n}(k), \quad (3.4)$$

where, at instant  $k$ ,  $\mathbf{x}(k) \in \Omega$  is the transmitted vector, and  $\mathbf{n}(k)$  is a Gaussian random vector with independent elements, zero mean, and variance  $N_0/2$  per dimension. Since  $\mathbf{x}(k)$  and  $\mathbf{y}(k)$  are both stationary processes, the argument  $k$  will be dropped from now on. All modulation schemes optimized for the AWGN or coherent optical systems can be used with IM/DD systems if they are DC-biased so that the signal driving the light source is nonnegative. However, these formats will not necessarily be optimized for the IM/DD channel too.

Barry [3, Ch. 5] reported the average optical power requirement of various modulation formats for IM/DD channels. This study included formats such as OOK,  $M$ -PAM, multilevel pulse-position modulation

( $M$ -PPM), and SCM formats such as  $M$ -PSK and  $M$ -QAM with a constant DC bias. These classical SCM formats which modulate a single carrier were shown to be less power efficient than other formats [3, Fig. 5.4]. In Ch. 4, the single-subcarrier modulation formats will be discussed in details.

This single-subcarrier modulation concept was also extended to many subcarriers as in the conventional electrical channel where the subcarriers can be superimposed resulting in a frequency-division multiplexing (FDM) system, referred to as multiple-subcarrier modulation (MSM) [3, p. 122], and orthogonal frequency-division multiplexing (OFDM) if the carriers are orthogonal [49]. Further, a subclass of OFDM known as discrete multitone (DMT), where the output of the inverse fast Fourier transform modulator is real instead of complex, has been investigated [50]. In [3, p. 134] and [51], the MSM was shown to have poor power efficiency compared to single-subcarrier modulation due to the increased required DC bias, and in [52], DMT was shown to considerably suffer in peak-power limited systems. In [53] and [10], different power reduction techniques have been investigated for MSM.

Lattice codes for IM/DD were investigated in [54] together with constellation shaping and nonequiprobable signaling. In [45], constellation shaping has been studied for IM/DD systems in the presence of optical amplification, which is outside the scope of this thesis. Hranilovic in [11] presented a signal space model for optical IM/DD channels where different basis functions were used to form the signals. These basis functions are, for example, the *prolate spheroidal* wave functions, *Walsh* functions denoted as adaptively-biased QAM (AB-QAM), and three one-dimensional rectangular pulse-shaped PAM symbols denoted as 3-D PAM. In addition, shaping regions to reduce the average and peak optical power were derived, and the performance of some lattice-based modulation formats, which are the result of intersecting a lattice with the shaping region, was reported.

In the next chapter, the signal space for single-subcarrier I/Q modulation formats over IM/DD channels will be introduced together with the figures of merit used to assess the different formats.

## Chapter 4

# Single-Subcarrier Noncoherent Modulation

The subcarrier modulation concept described in Sec. 3.2 allows the use of I/Q modulation formats with IM/DD channels provided that the signal is DC-biased to be nonnegative. In [7], the SCM concept with a constant bias was experimentally demonstrated, and in [55] and [8], a novel transmitter design for the subcarrier QPSK and 16-QAM was presented. Allowing the DC bias to vary on a symbol-by-symbol basis and within the symbol interval was shown to improve the power efficiency of SCM in [9] and [10], respectively. In [56], different 8-level SCM formats, with DC bias varying on a symbol-by-symbol basis, were experimentally demonstrated.

In this chapter, we will investigate the signal space introduced by Hranilovic [11] for single-subcarrier I/Q modulation formats which are compatible with IM/DD systems. This signal space will be taken into account together with the channel nonnegativity constraint to better design modulation formats which suit different power constraints that might be present in a communication system. Figures of merit which facilitate the comparison of the different modulation formats will be introduced together with the formulation of the constellation optimization problem. Finally, an example of the obtained results will be presented.

## 4.1 Single-Subcarrier Modulation Signal Space

Conventional I/Q modulation formats together with the added DC bias to guarantee nonnegativity can be translated geometrically by having a three-dimensional Euclidean space spanned by the orthonormal basis functions

$$\phi_1(t) = \sqrt{\frac{1}{T_s}} \operatorname{rect}\left(\frac{t}{T_s}\right), \quad (4.1)$$

$$\phi_2(t) = \sqrt{\frac{2}{T_s}} \cos(2\pi ft) \operatorname{rect}\left(\frac{t}{T_s}\right), \quad (4.2)$$

$$\phi_3(t) = \sqrt{\frac{2}{T_s}} \sin(2\pi ft) \operatorname{rect}\left(\frac{t}{T_s}\right), \quad (4.3)$$

where

$$\operatorname{rect}(t) = \begin{cases} 1, & \text{if } 0 \leq t \leq 1 \\ 0, & \text{otherwise} \end{cases},$$

and  $f$  is the electrical subcarrier frequency [11]. The basis function  $\phi_1(t)$  represents the DC bias, whereas  $\phi_2(t)$  and  $\phi_3(t)$  are the basis functions for the conventional I/Q modulation formats presented in Sec. 2.2 with rectangular pulse shaping. As in [3, pp. 115–116] and [7, 11], we use  $f = 1/T_s$ , which is the minimum value for which  $\phi_1(t)$ ,  $\phi_2(t)$ , and  $\phi_3(t)$  are orthonormal. These basis functions are depicted in Fig. 4.1.

The use of rectangular pulse shaping results in time-disjoint pulses, therefore, the criterion of having  $x(t)$  in (3.1) to be nonnegative can be simplified to having each of the signals  $s_i(t)$  in (2.2) belonging to the signaling set  $S$  to be nonnegative. Thus,  $s_{i,1}$  is chosen for each  $i = 0, \dots, M - 1$  such that

$$\min_t s_i(t) \geq 0,$$

which guarantees the nonnegativity of  $x(t)$  at all times. As a result, all the signals satisfying the nonnegativity constraint are confined to a region in the space spanned by  $\phi_1(t)$ ,  $\phi_2(t)$ , and  $\phi_3(t)$ . This region is known as the admissible region  $\Upsilon$  [11, Eq. (10)], and the constellation  $\Omega$  is a finite subset of  $\Upsilon$ . The admissible region for I/Q modulation

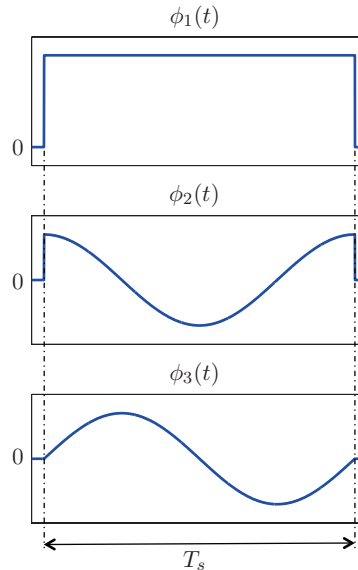


Figure 4.1: Single-subcarrier basis functions for IM/DD systems.

formats when used on IM/DD channels is

$$\Upsilon = \left\{ \mathbf{s} \in \mathbb{R}^3 : \min_{t \in [0, T_s)} \sum_{k=1}^3 s_{i,k} \phi_k(t) \geq 0 \right\}, \quad (4.4)$$

$$= \left\{ \mathbf{s} \in \mathbb{R}^3 : s_{i,1}^2 \geq 2(s_{i,2}^2 + s_{i,3}^2) \right\}, \quad (4.5)$$

which is a three-dimensional cone with vertex at the origin, apex angle of  $\cos^{-1}(1/3) = 70.528^\circ$ , and opening in the dimension spanned by  $\phi_1(t)$  [5, Fig. 4.2].

Fig. 4.2 shows an example of three modulation formats and how they fit in the admissible region  $\Upsilon$ . The first is the nonnegative 4-PAM constellation where all the constellation points, i.e., the coordinates of the sphere centers, are in the  $\phi_1(t)$  direction [3, Eq. (5.8)]. The diameter of the spheres represents the minimum distance between the constellation points. The second is the conventional 16-QAM where the points lie on three circles with different radii. All the signals of 16-QAM are equally biased such that all the constellation points belong to the admissible region, i.e., satisfying the nonnegativity constraint of the channel [3, Eq. (5.27)]. The last format is a version of 16-QAM

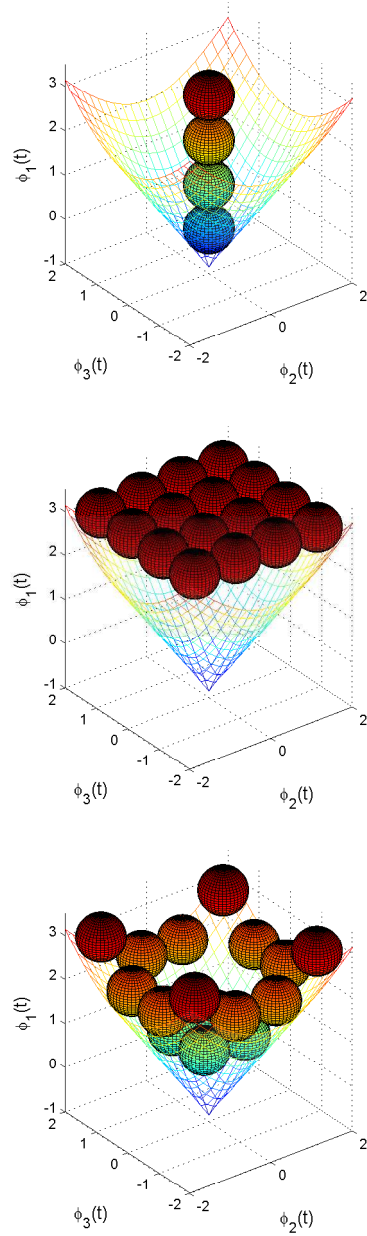


Figure 4.2: 4-PAM (top), 16-QAM (middle), and 16-QAM where the DC bias is different for different symbols (bottom).

denoted as  $\checkmark$ 16-QAM where every signal is biased with the minimum amount required to become nonnegative. This constellation is based on the work in [5, p. 78], [9] where the bias is assumed not to be fixed over all the transmitted symbols. Since the constellation points lying on each of the three circles constituting the 16-QAM constellation require a different DC bias, the three rings are not aligned at the same level in the direction spanned by  $\phi_1(t)$ . However, the coordinates of 16-QAM and  $\checkmark$ 16-QAM are the same in the plane spanned by  $\phi_2(t)$  and  $\phi_3(t)$ . Unlike the equally biased conventional 16-QAM, the DC bias for  $\checkmark$ 16-QAM carries information and thus can be used in the decision circuitry at the receiver. This modulation format is not optimized for a certain power measure; however, it leads to improved power efficiency compared to the 16-QAM when used over IM/DD channels.

## 4.2 Figures of Merit

Three different power measures can be extracted from the passband and baseband models in Fig. 3.3. The first entity is the average electrical power defined as

$$\bar{P}_e = \lim_{T \rightarrow \infty} \frac{1}{2T} \int_{-T}^T x^2(t) dt,$$

which for any set of basis functions can be simplified to

$$\bar{P}_e = \frac{E_s}{T_s} = \frac{1}{T_s} \mathbb{E}[\|\mathbf{s}_I\|^2], \quad (4.6)$$

where  $E_s$  is the average energy of the constellation,  $\mathbb{E}[\cdot]$  is the expected value, and  $I$  is a random variable uniformly distributed over  $\{0, 1, \dots, M-1\}$ . This entity is an important figure of merit for assessing the performance of digital communication systems [15, p. 40]. Therefore, it is relevant for IM/DD systems for compatibility with classical methods and results [57, 58]. In addition, it helps in quantifying the impact of relative intensity noise (RIN) in fiber-optical links [42], and in assessing the power consumption of optical systems [12].

The second measure is the average optical power  $\bar{P}_o$ , which has been studied in [3, 4, 11, 46, 47] for the wireless optical channel. Limitations are set on  $\bar{P}_o$  for skin- and eye-safety standards to be

met. In fiber-optic communications, this entity is used to quantify the impact of shot noise on the performance [42, p. 20]. It is defined as

$$\bar{P}_o = \lim_{T \rightarrow \infty} \frac{1}{2T} \int_{-T}^T z^2(t) dt = \lim_{T \rightarrow \infty} \frac{c}{2T} \int_{-T}^T x(t) dt.$$

This measure depends solely on the DC bias required to make the signals nonnegative and can be represented in terms of the symbol period and the constellation geometry as [11, 46]

$$\bar{P}_o = \frac{c}{\sqrt{T_s}} \mathbb{E}[s_{I,1}], \quad (4.7)$$

regardless of  $\phi_2(t)$  and  $\phi_3(t)$ .

The third measure is the peak optical power defined as

$$\hat{P}_o = \max_t \mathbb{L}\{z^2(t)\} \quad (4.8)$$

$$= \max_t \frac{z^2(t)}{2} \quad (4.9)$$

$$= c \max_t x(t) \quad (4.10)$$

$$= c \max_{i,t} s_i(t), \quad (4.11)$$

where (4.11) is valid for the time-disjoint signaling considered in this work. This entity gives a measure of tolerance against the nonlinear behavior of transmitting and receiving hardware in communication systems [11, 13, 44] and has been studied in [11, 47, 59].

For the IM/DD basis functions defined in Sec. 4.1, the peak optical power can be expressed as

$$\hat{P}_o = \frac{c}{\sqrt{T_s}} \max_i \left\{ s_{i,1} + \sqrt{2(s_{i,2}^2 + s_{i,3}^2)} \right\}, \quad (4.12)$$

for  $i = 0, \dots, M - 1$ .

As a possible fourth measure, one might consider the peak electrical power

$$\hat{P}_e = \max_t x^2(t).$$

However, it is directly related to  $\hat{P}_o$  by  $c^2 \hat{P}_e = \hat{P}_o^2$ , and will therefore not be considered further.

Fig. 4.3 depicts a contour plot of the three power measures in signal space together with the admissible region  $\Upsilon$ . This gives a better

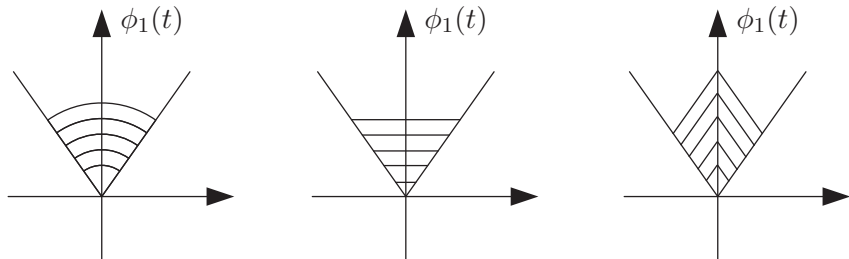


Figure 4.3: (left to right): Contours of equal average electrical power  $\bar{P}_e$ , average optical power  $\bar{P}_o$ , and peak optical power  $\hat{P}_o$ .

insight on which modulation formats are suitable for which power constraint that might be present in a certain IM/DD system.

To assess the performance of the different modulation formats in the presence of capacity-achieving error-correcting codes, we consider the mutual information [60, Sec. 2.4]

$$I(\mathbf{x}; \mathbf{y}) = H(\mathbf{x}) - H(\mathbf{x}|\mathbf{y}) \quad (4.13)$$

as a performance measure. It upperbounds the achievable rates  $R$  in information bits per symbol for virtually error-free communication in a coded system. The terms  $H(\mathbf{x})$  and  $H(\mathbf{x}|\mathbf{y})$  are the entropy of  $\mathbf{x}$  and the conditional entropy of  $\mathbf{x}$  given the received vector  $\mathbf{y}$ .

We define  $R_s = 1/T_s$  as the symbol rate in symbols per second, the bit rate  $R_b = R_s R$  in bits per second, and  $E_b = E_s/R$  as the average energy per bit. Furthermore, in order to have a fair comparison, the spectral efficiency defined as

$$\eta = \frac{R_b}{W} \text{ [bits/s/Hz]} \quad (4.14)$$

should be taken into account, where  $W$  is the baseband bandwidth defined as the first null in the spectrum of  $x(t)$ . At the same symbol rate, modulation formats such as OOK and  $M$ -PAM have  $W = R_s$ , whereas modulation formats belonging to the single-subcarrier family occupy  $W = 2R_s$  [Paper A, Fig. 2]. This is due to the intermediate step of modulating the information onto an electrical subcarrier before modulating the optical carrier [3, Ch. 5]. In our work, we are interested in

two extreme cases: the uncoded system, for which  $R = \log_2 M$ , and the system with optimal coding, for which  $R = I(\mathbf{x}; \mathbf{y})$ .

In [Paper C], the above figures of merit are used to evaluate the performance of previously known and newly obtained modulation formats.

### 4.3 Constellation Optimization

As opposed to biasing I/Q modulation formats with a constant bias, e.g., 16-QAM in Fig. 4.2 (middle), varying the bias on a symbol-by-symbol basis results in a better power efficiency, e.g., 16-QAM in Fig. 4.2 (bottom). However, it can be seen from Fig. 4.2 that there is still room for more power-efficient modulation formats. This is done by including the admissible region as a constraint in the optimization problem. As done before for the conventional AWGN channel [20–24], our approach of finding the best constellations is formulated as a sphere packing problem with the objective of minimizing the different power measures separately, whether it is average electrical, optical, or peak power.

Fig. 4.4 shows an example of the 4-level constellation which provides the lowest average electrical, optical, and peak power. The geometry of this constellation is a regular tetrahedron where all the spheres, or the constellation points lying at the vertices of this regular tetrahedron, are equidistant from each other and normalized to unit  $d_{\min}$ . This constellation is also a subset of the intersection between the admissible region  $\Upsilon$  and the face-centered cubic lattice, where the apex of the cone coincides with a lattice point and the lattice is oriented such that two lattice basis vectors lie in the plane spanned by  $\phi_2(t)$  and  $\phi_3(t)$ . For the 4-level constellation in Fig. 4.4, it is remarkable that the vertex angle of the tetrahedron, defined as the apex angle of the circumscribed cone, is exactly  $\cos^{-1}(1/3)$ , which is equal to the apex angle of the admissible region  $\Upsilon$ . Thus, this constellation fits  $\Upsilon$  snugly, in the sense that all constellation points, regarded as unit-diameter spheres, touch each other as well as the boundary of  $\Upsilon$ . This modulation format consists of a zero level signal and a biased ternary PSK [61, 62], and this can be seen in Fig. 4.5. Other hybrids between amplitude-shift keying and PSK have been studied in [63] and [64]; however, such modulation formats do not satisfy the

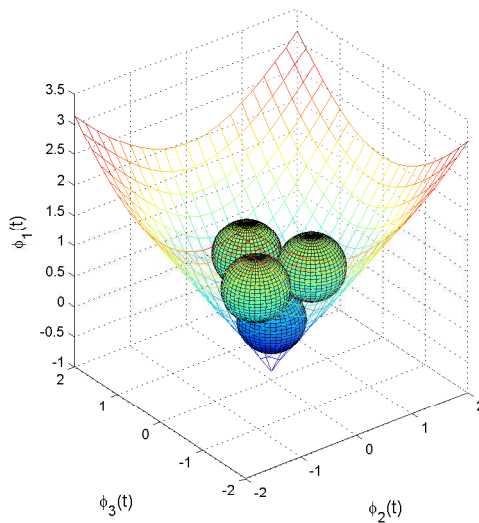


Figure 4.4: The obtained 4-level constellation which is optimized for average electrical, optical, and peak power.

nonnegativity constraint of IM/DD channels.

#### 4.4 Experimental Verification

In order to verify the theoretical results obtained about this 4-level modulation format, an experimental verification has been carried out in the lab. The setup is shown in Fig. 4.6 where the waveforms of this modulation format have been programmed in an arbitrary waveform generator. Its output  $x(t)$  is fed into a vertical-cavity surface-emitting laser (VCSEL) which is a type of semiconductor laser diode. The generated optical signal  $z(t)$  propagates through a multimode fiber (MMF) of varying length which is followed by a variable optical attenuator (VOA) to vary the optical power of the signal propagating through the fiber. At the receiver, the photodiode (PD) captures the optical signal resulting in a current, i.e., the electrical signal  $y(t)$ , which is proportional to the optical power incident upon it. This signal is sampled by an oscilloscope and processed offline. Fig. 4.7 depicts the constellation diagram of the received symbols in the back-

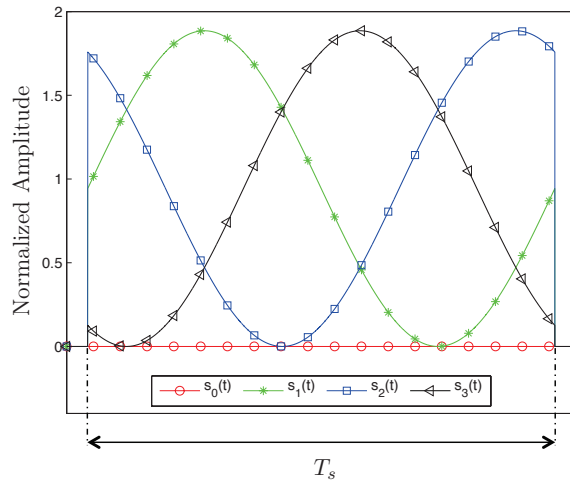


Figure 4.5: The 4-level constellation baseband waveforms over one symbol period.

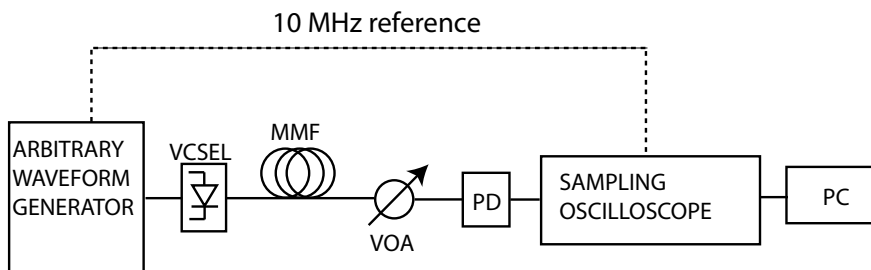


Figure 4.6: Experimental setup.

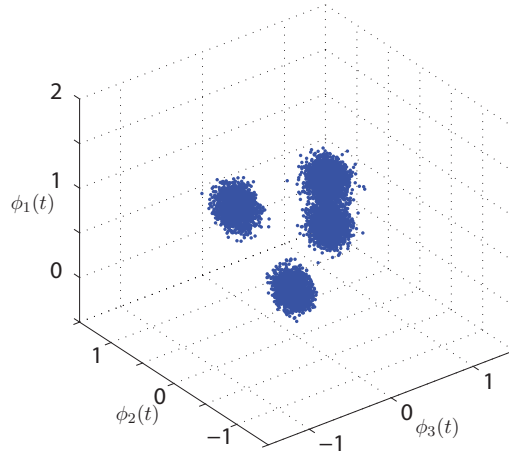


Figure 4.7: Experimental constellation diagram of the 4-level constellation in Fig. 4.4 in the back-to-back case.

to-back case, i.e., without transmission through a fiber medium. The results in [Paper B] show that the obtained 4-level modulation format in Fig. 4.4 is more power efficient in terms of average optical power than other formats with the same spectral efficiency at moderate to high SNR. However, this comes at the cost of having a higher transceiver complexity.

The conformity of the experimental results with the theoretical analysis led us to investigate higher-level modulation formats ( $M > 4$ ) with and without confining them to a lattice structure. A lattice-based constellation simplifies the transmitter and receiver due to the geometric regularity embedded in its structure. Therefore, we consider optimizing modulation formats where the set of constellation points belong to the face-centered cubic lattice which provides the densest packing for the three-dimensional Euclidean space [27, p. xvi]. In [Paper C], the performance of the different modulation formats is reported in the presence and absence of capacity-achieving error-correcting codes. Therefore, this work could serve as a guideline for which modulation formats to choose for a particular IM/DD system based on the trade-offs between power efficiency, spectral efficiency, and the cost/complexity required.

# Chapter 5

## Contributions

This chapter summarizes the contributions of the appended papers which fall in the category of optimizing modulation formats for IM/DD systems.

### 5.1 Included Publications

#### **Paper A: “Power efficient subcarrier modulation for intensity modulated channels”**

In this paper, we propose a novel quaternary subcarrier modulation scheme for IM/DD systems which is a hybrid between on-off keying and ternary phase-shift keying. At asymptotically high signal-to-noise ratios, this hybrid scheme has a 1.2 dB average electrical power gain and 0.6 dB average optical power gain compared to OOK, making it the most power-efficient format for IM/DD systems with a spectral efficiency of 1 bit/s/Hz. However, for systems that are limited by laser nonlinearities, we show that OOK is the best choice.

#### **Paper B: “Experimental comparison of modulation formats in IM/DD links”**

The idea behind this contribution is to complement the previously obtained theoretical results with experimental results. Therefore, we present an experimental comparison of modulation formats over IM/DD systems with a spectral efficiency of 1 bit/s/Hz. This includes OOK, subcarrier QPSK, and the hybrid modulation scheme

proposed in [Paper A]. The proposed modulation format is shown to be more power efficient in terms of average optical power compared to the other modulation formats under study at moderate to high SNR, and this is in agreement with the theoretical results. However, the gain comes at the cost of higher transceiver complexity. At low SNR, OOK has a better performance. We also study the impact of propagation in multimode fibers, where the conclusion is that the modulation formats have a similar performance penalty due to the modal dispersion.

### **Paper C: “Optimizing constellations for noncoherent optical communication systems”**

In this paper, we propose a set of 4-, 8-, and 16-level single-subcarrier modulation formats for IM/DD systems which are optimized for average electrical, average optical, and peak power. The overall gain compared to the previously best known formats ranges from 0.6 dB to 3 dB in the absence of error-correcting codes. An interesting observation is that modulation formats optimized for peak power perform well also in average-power limited systems. We also analyze the performance of the obtained modulation formats in terms of mutual information, in order to predict their performance in the presence of capacity-achieving error-correcting codes. The gain of the obtained formats ranges from 0.3 dB to 1 dB. Finally, we analytically optimize modulation formats which require the least energy per bit in the low SNR regime and compare them with the other obtained modulation formats.

## **5.2 Other Contributions**

Below are other contributions by the author which are not included in this thesis, either due to content overlap with the appended papers, or due to content which is not related to this thesis.

[P1] **J. Karout**, K. Szczerba, and E. Agrell, “Modulation scheme,” U.S. Patent Application No. 12/976,188, Unpublished (filing date Dec. 22, 2010).

[C7] **J. Karout**, E. Agrell, K. Szczerba, and M. Karlsson, “Designing power-efficient modulation formats for noncoherent optical

- systems,” in *Proc. IEEE Global Communications Conference*, 2011.
- [C6] M. Tavan, E. Agrell, and **J. Karout**, “Strictly bandlimited ISI-free transmission over intensity-modulated channels,” in *Proc. IEEE Global Communications Conference*, 2011.
- [C5] K. Szczerba, **J. Karout**, E. Agrell, P. Westbergh, M. Karlsson, P. Andrekson, and A. Larsson, “Demonstration of 8-level sub-carrier modulation sensitivity improvement in an IM/DD system,” in *Proc. European Conference and Exhibition on Optical Communication*, 2011.
- [C4] K. Szczerba, P. Westbergh, J. Gustavsson, Å. Haglund, **J. Karout**, M. Karlsson, P. Andrekson, E. Agrell, and A. Larsson, “30 Gbps 4-PAM transmission over 200m of MMF using an 850 nm VCSEL,” in *Proc. European Conference and Exhibition on Optical Communication*, 2011.
- [C3] N. Jiang, Y. Gong, **J. Karout**, H. Wymeersch, P. Johannisson, M. Karlsson, E. Agrell, and P. A. Andrekson, “Stochastic back-propagation for coherent optical communications,” in *Proc. European Conference and Exhibition on Optical Communication*, 2011.
- [C2] **J. Karout**, H. Wymeersch, A. S. Tan, P. Johannisson, E. Agrell, M. Sjödin, M. Karlsson, and P. Andrekson, “CMA misconvergence in coherent optical communication for signals generated from a single PRBS,” in *Proc. Wireless and Optical Communications Conference*, 2011.
- [C1] **J. Karout**, L. S. Muppisetty, and T. Svensson, “Performance trade-off investigation of B-IFDMA,” in *Proc. IEEE Vehicular Technology Conference Fall*, 2009.

## References

- [1] C. E. Shannon, "A mathematical theory of communication," *Bell System Technical Journal*, vol. 27, pp. 379–423 and 623–656, 1948.
- [2] G. P. Agrawal, *Lightwave Technology: Telecommunication Systems*. New Jersey: John Wiley & Sons, Inc., 2005.
- [3] J. R. Barry, *Wireless Infrared Communications*. Norwell, MA, USA: Kluwer Academic Publishers, 1994.
- [4] J. M. Kahn and J. R. Barry, "Wireless infrared communications," *Proceedings of the IEEE*, vol. 85, no. 2, pp. 265–298, 1997.
- [5] S. Hranilovic, *Wireless Optical Communication Systems*. New York: Springer, 2005.
- [6] P. J. Winzer and R.-J. Essiambre, "Advanced optical modulation formats," *Proceedings of the IEEE*, vol. 94, no. 5, pp. 952–985, 2006.
- [7] A. O. J. Wiberg, B.-E. Olsson, and P. A. Andrekson, "Single cycle subcarrier modulation," in *Proc. Optical Fiber Communication Conference*, 2009, p. OTuE1.
- [8] B.-E. Olsson and M. Sköld, "QPSK transmitter based on optical amplitude modulation of electrically generated QPSK signal," in *Proc. Asia Optical Fiber Communication and Optoelectronic Exposition and Conference*, 2008, p. SaA3.
- [9] S. Hranilovic and D. A. Johns, "A multilevel modulation scheme for high-speed wireless infrared communications," in *Proc. IEEE International Symposium on Circuits and Systems*, 1999, pp. 338–341.
- [10] R. You and J. M. Kahn, "Average power reduction techniques for multiple-subcarrier intensity-modulated optical signals," *IEEE Transactions on Communications*, vol. 49, no. 12, pp. 2164–2171, 2001.

- 
- [11] S. Hranilovic and F. R. Kschischang, "Optical intensity-modulated direct detection channels: Signal space and lattice codes," *IEEE Transactions on Information Theory*, vol. 49, no. 6, pp. 1385–1399, 2003.
- [12] L. P. Chen and K. Y. Lau, "Regime where zero-bias is the low-power solution for digitally modulated laser diodes," *IEEE Photonics Technology Letters*, vol. 8, no. 2, pp. 185–187, 1996.
- [13] B. Inan, S. C. J. Lee, S. Randel, I. Neokosmidis, A. M. J. Koonen, and J. W. Walewski, "Impact of LED nonlinearity on discrete multitone modulation," *Journal of Optical Communications and Networking*, vol. 1, no. 5, pp. 439–451, Oct. 2009.
- [14] J. G. Proakis, *Digital Communications*, 3rd ed. McGraw-Hill, 1995.
- [15] M. K. Simon, S. M. Hinedi, and W. C. Lindsey, *Digital Communication Techniques: Signal Design and Detection*. Englewood Cliffs, NJ: Prentice-Hall, 1995.
- [16] V. A. Kotelnikov, "The theory of optimum noise immunity," Ph.D. dissertation, Molotov Energy Institute, Moscow, 1947.
- [17] J. M. Wozencraft and I. M. Jacobs, *Principles of Communication Engineering*. New York: John Wiley & Sons, Inc., 1965.
- [18] J. B. Anderson, *Digital Transmission Engineering*, 2nd ed. New Jersey: IEEE Press, 2005.
- [19] S. Haykin, *Communication Systems*, 4th ed. New York: John Wiley & Sons, Inc., 2001.
- [20] G. Foschini, R. Gitlin, and S. Weinstein, "Optimization of two-dimensional signal constellations in the presence of Gaussian noise," *IEEE Transactions on Communications*, vol. COM-22, no. 1, pp. 28–38, Jan. 1974.
- [21] J.-E. Porath and T. Aulin, "Design of multidimensional signal constellations," *IEE Proceedings - Communications*, vol. 150, no. 5, pp. 317–323, Oct. 2003.

- [22] N. J. A. Sloane, R. H. Hardin, T. D. S. Duff, and J. H. Conway, "Minimal-energy clusters of hard spheres," *Discrete and Computational Geometry*, vol. 14, no. 3, pp. 237–259, 1995.
- [23] R. L. Graham and N. J. A. Sloane, "Penny-packing and two-dimensional codes," *Discrete and Computational Geometry*, vol. 5, no. 1, pp. 1–11, 1990.
- [24] E. Agrell and M. Karlsson, "Power-efficient modulation formats in coherent transmission systems," *Journal of Lightwave Technology*, vol. 27, no. 22, pp. 5115–5126, 2009.
- [25] G. D. Forney, Jr., "Coset codes—Part I: Introduction and geometrical classification," *IEEE Transactions on Information Theory*, vol. 34, no. 5, pp. 1123–1151, 1988.
- [26] G. D. Forney, Jr. and L.-F. Wei, "Multidimensional constellations—Part I. Introduction, figures of merit, and generalized cross constellations," *IEEE Journal on Selected Areas in Communications*, vol. 7, no. 6, pp. 877–892, 1989.
- [27] J. H. Conway and N. J. A. Sloane, *Sphere Packings, Lattices and Groups*, 3rd ed. New York: Springer-Verlag, 1999.
- [28] E. Specht, "The best known packings of equal circles in the unit circle," 2009. [Online]. Available: <http://hydra.nat.uni-magdeburg.de/packing/cci/cci.html>
- [29] M. Karlsson and E. Agrell, "Power-efficient modulation schemes," in *Impact of Nonlinearities on Fiber Optic Communications*, S. Kumar, Ed. Springer, 2011, ch. 5, pp. 219–252.
- [30] K. C. Kao and G. A. Hockham, "Dielectric-fibre surface waveguides for optical frequencies," *Proceedings of the Institution of Electrical Engineers*, vol. 113, no. 7, pp. 1151–1158, Jul. 1966.
- [31] F. R. Gfeller and U. Bapst, "Wireless in-house data communication via diffuse infrared radiation," *Proceedings of the IEEE*, vol. 67, no. 11, pp. 1474 – 1486, Nov. 1979.
- [32] H. Sun, K.-T. Wu, and K. Roberts, "Real-time measurements of a 40 Gb/s coherent system," *Optics Express*, vol. 16, no. 2, pp. 873–879, Jan. 2008.

- [33] M. Seimetz, “Multi-format transmitters for coherent optical M-PSK and M-QAM transmission,” in *Proc. 7th International Conference on Transparent Optical Networks*, 2005, pp. 225–229.
- [34] J. P. Gordon, L. R. Walker, and W. H. Louisell, “Quantum statistics of masers and attenuators,” *Physical Review*, vol. 130, no. 2, pp. 806–812, Apr. 1963.
- [35] J. M. Kahn and K.-P. Ho, “Spectral efficiency limits and modulation/detection techniques for DWDM systems,” *IEEE Journal of Selected Topics in Quantum Electronics*, vol. 10, no. 2, pp. 259–272, Mar./Apr. 2004.
- [36] E. Ip, A. P. T. Lau, D. J. F. Barros, and J. M. Kahn, “Coherent detection in optical fiber systems,” *Optics express*, vol. 16, no. 2, pp. 753–791, Jan. 2008.
- [37] S. Betti, F. Curti, G. De Marchis, and E. Iannone, “Exploiting fibre optics transmission capacity: 4-quadrature multilevel signalling,” *Electronics Letters*, vol. 26, no. 14, pp. 992–993, Jul. 1990.
- [38] —, “A novel multilevel coherent optical system: 4-quadrature signaling,” *Journal of Lightwave Technology*, vol. 9, no. 4, pp. 514–523, Apr. 1991.
- [39] S. Betti, G. De Marchis, E. Iannone, and P. Lazzaro, “Homodyne optical coherent systems based on polarization modulation,” *Journal of Lightwave Technology*, vol. 9, no. 10, pp. 1314–1320, Oct. 1991.
- [40] R. Cusani, E. Iannone, A. M. Salonic, and M. Todaro, “An efficient multilevel coherent optical system: M-4Q-QAM,” *Journal of Lightwave Technology*, vol. 10, no. 6, pp. 777–786, Jun. 1992.
- [41] S. Randel, F. Breyer, and S. C. J. Lee, “High-speed transmission over multimode optical fibers,” in *Proc. Optical Fiber Communication Conference*, 2008, p. OWR2.
- [42] C. Cox and W. S. C. Chang, “Figures of merit and performance analysis of photonic microwave links,” in *RF Photonic Technology in Optical Fiber Links*, W. S. C. Chang, Ed. Cambridge University Press, 2002, ch. 1, pp. 1–33.

- [43] P. Westbergh, J. S. Gustavsson, Å. Haglund, A. Larsson, F. Hopfer, G. Fiol, D. Bimberg, and A. Joel, “32 Gbit/s multimode fibre transmission using high-speed, low current density 850 nm VCSEL,” *Electronics Letters*, vol. 45, no. 7, pp. 366–368, 2009.
- [44] L. A. Coldren and E. R. Hegblom, “Fundamental issues in VCSEL design,” in *Vertical-Cavity Surface-Emitting Lasers: Design, Fabrication, Characterization, and Applications*, C. W. Wilmsen, H. Temkin, and L. A. Coldren, Eds. Cambridge University Press, 1999, ch. 2, pp. 32–67.
- [45] W. Mao and J. M. Kahn, “Lattice codes for amplified direct-detection optical systems,” *IEEE Transactions on Communications*, vol. 56, no. 7, pp. 1137–1145, 2008.
- [46] S. Hranilovic and F. R. Kschischang, “Capacity bounds for power- and band-limited optical intensity channels corrupted by Gaussian noise,” *IEEE Transactions on Information Theory*, vol. 50, no. 5, pp. 784–795, 2004.
- [47] A. A. Farid and S. Hranilovic, “Capacity bounds for wireless optical intensity channels with Gaussian noise,” *IEEE Transactions on Information Theory*, vol. 56, no. 12, pp. 6066–6077, 2010.
- [48] A. Lapidoth, S. M. Moser, and M. A. Wigger, “On the capacity of free-space optical intensity channels,” *IEEE Transactions on Information Theory*, vol. 55, no. 10, pp. 4449–4461, Oct. 2009.
- [49] J. Armstrong, “OFDM for optical communications,” *Journal of Lightwave Technology*, vol. 27, no. 3, pp. 189–204, Feb. 2009.
- [50] S. C. J. Lee, F. Breyer, S. Randel, H. P. A. van den Boom, and A. M. J. Koonen, “High-speed transmission over multimode fiber using discrete multitone modulation,” *Journal of Optical Networking*, vol. 7, no. 2, pp. 183–196, Feb. 2008.
- [51] J. B. Carruthers and J. M. Kahn, “Multiple-subcarrier modulation for nondirected wireless infrared communication,” *IEEE Journal on Selected Areas in Communications*, vol. 14, no. 3, pp. 538–546, Apr. 1996.

- [52] S. Randel, F. Breyer, S. C. J. Lee, and J. W. Walewski, "Advanced modulation schemes for short-range optical communications," *IEEE Journal of Selected Topics in Quantum Electronics*, vol. 16, no. 5, pp. 1280–1289, Sep./Oct. 2010.
- [53] W. Kang and S. Hranilovic, "Optical power reduction for multiple-subcarrier modulated indoor wireless optical channels," in *Proc. IEEE International Conference on Communications*, 2006, pp. 2743–2748.
- [54] D.-S. Shiu and J. M. Kahn, "Shaping and nonequiprobable signaling for intensity-modulated signals," *IEEE Transactions on Information Theory*, vol. 45, no. 7, pp. 2661–2668, 1999.
- [55] B.-E. Olsson and A. Alping, "Electro-optical subcarrier modulation transmitter for 100 GbE DWDM transport," in *Proc. Asia Optical Fiber Communication and Optoelectronic Exposition and Conference*, 2008, p. SaF3.
- [56] K. Szczerba, J. Karout, E. Agrell, P. Westbergh, M. Karlsson, P. Andrekson, and A. Larsson, "Demonstration of 8-level subcarrier modulation sensitivity improvement in an IM/DD system," in *Proc. European Conference and Exhibition on Optical Communication*, 2011.
- [57] K.-P. Ho, "Exact evaluation of the capacity for intensity-modulated direct-detection channels with optical amplifier noises," *IEEE Photonics Technology Letters*, vol. 17, no. 4, pp. 858–860, Apr. 2005.
- [58] M. S. Moreolo, R. Muñoz, and G. Junyent, "Novel power efficient optical OFDM based on Hartley transform for intensity-modulated direct-detection systems," *Journal of Lightwave Technology*, vol. 28, no. 5, pp. 798–805, Mar. 2010.
- [59] J. Karout, E. Agrell, and M. Karlsson, "Power efficient subcarrier modulation for intensity modulated channels," *Optics Express*, vol. 18, no. 17, pp. 17913–17921, Aug. 2010.
- [60] T. M. Cover and J. A. Thomas, *Elements of Information Theory*, 2nd ed. New Jersey: John Wiley & Sons, Inc., 2006.

- 
- [61] J. R. Pierce, "Comparison of three-phase modulation with two-phase and four-phase modulation," *IEEE Transactions on Communications*, vol. COM-28, no. 7, pp. 1098–1099, 1980.
  - [62] N. Ekanayake and T. T. Tjhung, "On ternary phase-shift keyed signaling," *IEEE Transactions on Information Theory*, vol. IT-28, no. 4, pp. 658–660, Jul. 1982.
  - [63] R.-J. Essiambre, G. Kramer, P. J. Winzer, G. J. Foschini, and B. Goebel, "Capacity limits of optical fiber networks," *Journal of Lightwave Technology*, vol. 28, no. 4, pp. 662–701, Feb. 2010.
  - [64] M. C. Gursoy, "Error rate analysis for peaky signaling over fading channels," *IEEE Transactions on Communications*, vol. 57, no. 9, pp. 2546–2550, Sep. 2009.